Air pollution weakens global spring greening

Chaoyang Wu (wucy@igsnrr.ac.cn)
Institute of Geographic Sciences and Natural Resources Research https://orcid.org/0000-0001-6163-8209

Hao Hua
Chinse Academy Sciences

Jian Wang
The Ohio State University

Lingwen Dong
Chinese Academy Sciences

Constantin Zohner
ETH Zurich https://orcid.org/0000-0002-8302-4854

Josep Penuelas
CSIC, Global Ecology Unit CREAF-CSIC-UAB, Cerdanyola del Vallès 08193, Catalonia, Spain
https://orcid.org/0000-0002-7215-0150

Yunqi Wang
Beijing Forestry University

Yuyu Zhou
The University of Hong Kong https://orcid.org/0000-0003-1765-6789

Shushi Peng
Peking University https://orcid.org/0000-0001-5098-726X

Zaichun Zhu
Peking University https://orcid.org/0000-0001-5235-5194

Jing Wei
University of Maryland, College Park

Wenping Yuan
Cold and Arid Regions Environmental and Engineering Research Institute, Chinese Academy of Sciences

Xiuzhi Chen
School of Atmospheric Sciences, Sun Yat-sen University https://orcid.org/0009-0003-5688-2997

Lei Chen
Sichuan University https://orcid.org/0000-0001-7011-8782

Yongshuo Fu
Beijing Normal University

Jialing Li
Nanjing University

Weimin Ju
Nanjing University https://orcid.org/0000-0002-0010-7401
Yanlian Zhou
Nanjing University
Dan Liang
Agricultural Information Institute of CAAS
Pierre Friedlingstein
University of Exeter https://orcid.org/0000-0003-3309-4739
Stephen Sitch
University of Exeter https://orcid.org/0000-0003-1821-8561
Yuming Guo
Monash University https://orcid.org/0000-0002-1766-6592
Quansheng Ge
geqs@igsnrr.ac.cn https://orcid.org/0000-0001-8712-8565

Biological Sciences - Article

Keywords:

Posted Date: February 2nd, 2024

DOI: https://doi.org/10.21203/rs.3.rs-3868370/v1

Additional Declarations: There is **NO** Competing Interest.

Abstract

Climate change is causing widespread land surface greening in spring1–4, but the impacts of anthropogenic air pollution on these changes remain poorly understood. Using global ground and satellite observations of fine particulate matter ≤ 2.5 μm (PM2.5) from 2000 to 2020, here we show that PM2.5 concentration offsets global spring greening as indicated by significant decreases in the normalized difference vegetation index (NDVI), leaf area index (LAI), and solar-induced fluorescence (SIF). Our experiments and meta-analyses involving up to 104 worldwide species reveal that pollution-induced greenness declines are primarily due to physical blockage and damage to leaf stomata. However, factors such as increased diffuse radiation and nitrogen deposition may occasionally enhance greening. Moreover, we observed significant variations among state-of-art terrestrial ecosystem models in replicating these greenness declines, with incorrect representation of PM2.5 effects on vegetation greening for roughly one third of global land coverage, further underscoring the importance of empirical data for benchmarking these models. This study reveals the negative feedback between anthropogenic air pollution and terrestrial carbon uptake, emphasizing the critical need for major polluting countries to mitigate air pollution and CO2 emissions.

Main

The ongoing climate change is causing significant changes to the terrestrial surface of the Earth[5]. As atmospheric CO_2 concentrations rise, understanding the impact of climate change on photosynthetic activity becomes critical to comprehending and predicting the future carbon cycle[6–8]. Climate warming has increased the carbon uptake potential of terrestrial ecosystems[9] by increasing plant activity through elevated CO_2 levels and nitrogen deposition[1,2] and through inducing earlier leaf onset in spring[10–12]. Greening of the terrestrial surface has therefore been observed worldwide over recent decades[13]. However, there are still poorly understood mechanisms that might counteract global greening trends and increases in plant photosynthesis, such as air pollution, that pose significant challenges to predicting future vegetation activity and carbon uptake. One of the major challenges with air pollution is the large increase in the emissions of fine particulate matter ($PM_{2.5}$), particularly due to rapidly growing cities with unprecedented urbanization[14,15] as well as increased wildfires globally[16,17]. $PM_{2.5}$ pollution adversely affects human health[18], but its effects on ecosystems, particularly on land surface greening and carbon uptake in spring, are not well understood.

While it is well established that human activities have a significant impact on ecosystem processes[19], the extent to which $PM_{2.5}$ pollutants emitted globally over the past two decades have affected vegetation activity remains unknown. Due to its properties, including scattering mass efficiency and optical hygroscopicity, $PM_{2.5}$ pollution can alter the propagation of visible light and significantly reduce atmospheric visibility[17], making it likely to have a strong effect on spring greening and vegetation activity through both biogeophysical and biochemical paths. To investigate this, we used a large-scale

monitoring network that collected ground-sourced observations of $PM_{2.5}$ emissions at 3580 sites, as well as satellite records spanning 2000-2020[20] (Extended data Fig. 1 and Supplementary Table 1 and Fig. 1). We combined this data with moderate-resolution satellite data on the normalized difference vegetation index (NDVI), leaf area index (LAI)[21], solar-induced fluorescence (SIF)[22], and climate to quantify the effects of $PM_{2.5}$ emissions on spring greening and vegetation activity. We then studied the underlying mechanisms of the observed trends using experimental data on leaf morphology from 15 tree species (Supplementary Table 2), meta-analytical data from 104 worldwide species (Supplementary Table 3), and global flux measurements from 187 sites representing various plant functional types and ecosystem characteristics (Supplementary Table 4). Lastly, we examined the $PM_{2.5}$ effects on spring productivity using 16 state-of-art terrestrial ecosystem models (Supplementary Table 5).

Results

We tested for the effects of $PM_{2.5}$ pollution and climate change on satellite-observed spring greenness (NDVI, LAI, and SIF) through rigorous analysis of ground and satellite data (Supplementary Materials and Methods). Before that, we first examined and minimized the attenuation effects of $PM_{2.5}$ pollution on the greenness signals of satellite observation (Supplementary Figs. 2 and 3). For the global scale, spatially explicit results for NDVI, LAI and SIF using satellite-based $PM_{2.5}$ pollution were provided (Fig. 1 B-D). $PM_{2.5}$ pollution led to reduced spring greening in 59.7-64.9% of the studied area, with 12.2-14.3% being significant. In comparison, $PM_{2.5}$ pollution led to increased spring greening in ~38% of regions (e.g., west Australia, North Africa, high lands in the northern Europe), with only ~4% being statistically significant. Consistent results were observed for the USA, Europe and China where ground monitoring networks have been well established. The ground-sourced observations demonstrate that $PM_{2.5}$ pollution were associated with decreased spring greening, with median standard sensitives for NDVI, LAI and SIF of -0.33, -0.36 and -0.38, respectively (Fig. 1 A).

We further conducted analyses to separate the greening effects of CO_2, temperature, precipitation, vapor pressure deficit (VPD), and $PM_{2.5}$ (Fig. 1 E-F). Stepwise regression analysis confirmed the dominant negative impacts of $PM_{2.5}$ pollution on spring greening at site and global scales, the extent of which was comparable to the inhibiting effects of vapor pressure deficit (Extended Data Figs. 2 and 3). Given the potential multicollinearity of driving factors, we also used partial correlation and ridge regression analyses and found consistently and dominantly negative effects of $PM_{2.5}$ pollution on spring greening (Extended Data Fig. 4 and Supplementary Fig. 4). Overall, these findings reveal that $PM_{2.5}$ pollution inhibits photosynthesis and offsets the ongoing trends in land surface greening globally.

To study the underlying mechanisms that drive the observed reductions in spring vegetation activity in response to $PM_{2.5}$ pollution, we conducted experiments on the leaf morphology of 15 widely-distributed tree species. We found that $PM_{2.5}$ can adhere to the leaf surface to varying degrees (Supplementary Fig. 5), potentially causing blockages and damage to leaf stomata, as observed through scanning electron

microscopy (Fig. 2A1-A15). To further investigate the effects of $PM_{2.5}$ on gas exchange and photosynthesis, including stomatal size, density and conductance, transpiration rate, chlorophyll content, maximum CO_2 assimilation rate, potential photosynthetic capacity (F_v/F_m), and photosynthetic rate, we conducted a meta-analysis based on 233 records of both experimental and observational results across 104 plant species worldwide (Fig. 2B). Overall, $PM_{2.5}$ exposure caused substantial reductions in stomatal size (−0.15, $P < 0.01$), stomatal conductance (−0.18, $P < 0.01$), chlorophyll content (−0.17, $P < 0.01$), transpiration rate (−0.27, $P < 0.01$), and photosynthetic rate (−0.18, $P < 0.01$). Similar results were found when separately analyzing the experimental and observational data (Supplementary Fig. 6). Notably, the significant decline in stomatal conductance and photosynthetic rate was identified as the key link between plant growth and $PM_{2.5}$ pollution. Further analysis of the effects of $PM_{2.5}$ on stomatal conductance using global flux measurements showed consistent results with the meta-analysis, indicating that increased $PM_{2.5}$ caused significant ($P < 0.05$) decreases in stomatal conductance and vegetation productivity accordingly (Fig. 2C and Supplementary Figs. 7 and 8). In line with flux measurements, $PM_{2.5}$ pollution could lower canopy stomatal conductance and SIF based on gridded data, supporting that $PM_{2.5}$ effects on greening trends are linked with the gas exchange between air and the interior of leaf (Supplementary Fig. 9).

To gain deeper insights into the underlying mechanisms that drive the correlation between $PM_{2.5}$ pollution and spring greening, we explored potential biogeophysical and biogeochemical paths for the correlation (Fig. 3). We found that elevated levels of $PM_{2.5}$ greatly reduced the amount of photosynthetically active radiation (PAR), with 64.7% of the grids showing a negative $PM_{2.5}$-PAR correlation (16.2% of which were significant). In line with gridded data analysis, flux measurements confirmed the negative impacts of $PM_{2.5}$ on PAR (Supplementary Fig. 10). This adverse effect on photosynthesis led to substantial declines in the maximum rate of carboxylation (VC_{max}), a key indicator of leaf photosynthetic capacity. This was evidenced by 64.1% negative correlations (12.3% significant) compared to only 35.9% positive correlations (3.6% significant). Since VC_{max} generally showed a positive correlation with SIF (62.0% positive vs. 1.2% negative, $P < 0.05$), higher $PM_{2.5}$ levels counteracted the process of spring greening (Fig. 3A). Similar trends were observed for LAI. Nonetheless, certain regions exhibited increased spring greening with higher $PM_{2.5}$. In these areas, $PM_{2.5}$ raised the fraction of diffuse radiation (PAR_{diff}/PAR) and nitrogen deposition ($N_{deposition}$). Our structural equation models supported the hypothesis that $PM_{2.5}$ decreased radiation, thereby reducing VC_{max} and LAI, but increased the fraction of diffuse radiation and $N_{deposition}$ (Fig. 3 C-H). Increased $PM_{2.5}$ concentration could also lower the ambient ozone (O_3) levels in spring due to lower atmospheric radiation, potentially undermining vegetation photosynthetic activities (Extended data Fig. 5). We also tested the impact of $PM_{2.5}$ on air temperature and found no dominant relationship (Supplementary Fig. 11), suggesting $PM_{2.5}$ pollution effect was not determined by air temperature regulation.

In a last step, we used the output from the TRENDY project to test the potential of 16 state-of-art terrestrial ecosystem models to reproduce the effects of $PM_{2.5}$ on gross primary productivity (GPP), a

productivity-based indicator of greening (Supplementary Table 5). Overall, the ecosystem models captured the widespread and negative effects of $PM_{2.5}$ (Fig. 4A and Supplementary Fig. 12). The standard sensitivity of GPP to $PM_{2.5}$ across the models was -0.15 ± 0.05, which is comparable with the inhibiting effects of VPD (Fig. 4B). However, the large biases of $PM_{2.5}$ effects, indicated by relatively high standard deviation of $PM_{2.5}$ sensitivity among models, were detected in the central of Europe and the eastern of America (Fig. 4C), suggesting the large inconsistency and limitation of model projections. Pixel-to-pixel comparison of $PM_{2.5}$ sensitivities between satellite observations and model projections suggests an incorrect representation of $PM_{2.5}$ effects on vegetation greening in nearly 34% of areas (Fig. 4D), highlighting the need for incorporating $PM_{2.5}$ effects into future model improvement.

Discussion

This study discovered and quantified the adverse effects of $PM_{2.5}$ air pollution on global spring greening trends over the past two decades. The findings reveal that ambient $PM_{2.5}$ pollution has had a negative impact on spring greenness and carbon uptake, as it has offset global change-induced greening. These results deepen our understanding of the impacts of human activities, including economic and social developments, on regional ecosystem functioning and its consequences for climate change. Given that high concentrations of $PM_{2.5}$ are closely linked with industrialization and urbanization[16,17], these results have important implications for the disparities across population and income groups[23] and emphasize the need for urgent action to reduce air pollution and greenhouse gas emissions in order to mitigate the negative impacts of human activity on the environment.

We identified specific mechanisms that explain how $PM_{2.5}$ contamination leads to a decrease in spring greening. We suggest that the key factor through which $PM_{2.5}$ affects photosynthesis appears to be the regulation of leaf stomata[24,25]. High concentrations of $PM_{2.5}$ can adsorb harmful substances such as SO_4^{2-}, NO^{3-}, and NH^{4+}, which can be detrimental to leaf growth[26,27]. Our results are supported by global flux data, an analysis of leaf morphology changes in 15 tree species, and a meta-analysis on 104 worldwide species which showed that $PM_{2.5}$ exposure significantly decreases stomatal conductance and photosynthetic rates. We also observed a significant decrease in the maximum rate of carboxylation, which is the single most important driver of leaf photosynthetic capacity, and which explains the declines in spring greenness and photosynthesis under high air pollution. These findings are consistent with the reported role of stomatal conductance in regulating photosynthesis[28].

We also identified additional factors contributing to the decline in spring greening due to $PM_{2.5}$ pollution. The significant reduction in radiation is likely to further contribute to the decreased greening observed in our study[29,30]. Lower radiation is closely tied to declines in the capacity for photosynthesis, represented here by the maximum rate of carboxylation (VC_{max}), leading to declines in LAI and SIF. Our results also indicated that $PM_{2.5}$ pollution contributed to enhanced greening in several regions. This positive effect is likely due to the increased fraction of diffuse radiation, elevated nitrogen deposition, and reduced risk of

O_3 exposure, which can boost plant photosynthesis and carbon storage[31,32]. For instance, nitrogen oxides (NO_x) associated with $PM_{2.5}$ pollution can promote nitrogen deposition[33]. Ecosystem models projected an overall negative correlation between $PM_{2.5}$ and spring Gross Primary Productivity (GPP), confirming the widespread adverse effects of $PM_{2.5}$ emissions on spring greening. Despite these findings, the limitations in accurately reproducing spatial patterns in $PM_{2.5}$ effects highlight the need for a more accurate representation of the impacts of air pollution in terrestrial ecosystem models.

In summary, our research forecasts that if air pollution, particularly $PM_{2.5}$, is not adequately managed, it will impede spring greening in the future, countering the current trends of global greening. This is especially critical for regions with high levels of $PM_{2.5}$ emissions, where immediate action to reduce air pollution is necessary. The effectiveness of these measures will be evident in the mitigation of the negative impact on spring greening, an essential factor in reducing CO_2 emissions through the photosynthesis of terrestrial ecosystems. Our results have important implications for policy design and implementation, as they highlight the synergies and trade-offs among various policies aimed at achieving sustainable development, especially in the context of social equity and climate change. Furthermore, our study underscores the impacts of aerosols, particularly $PM_{2.5}$, on climate change and highlights the uncertainties associated with future warming[34,35]. The detrimental influence of atmospheric pollution on spring greening reveals a critical feedback mechanism through which anthropogenic pollution may reduce the terrestrial carbon sink, further accelerating climate change. This underscores the critical importance of promoting sustainable development on a global scale.

Declarations

Acknowledgments: This work was funded by the National Natural Science Foundation of China (42125101) and the CAS Interdisciplinary Innovation Team (JCTD-2020-05). J.P. was funded by European Research Council Synergy grant ERC-SyG-2013-610028 IMBALANCE-P. J.P. was also financially supported by the Fundación Ramon Areces grant ELEMENTAL-CLIMATE, the Spanish Government grant PID2019-110521GB-I00, and the Catalan Government grant SGR 2017-1005. C.M.Z. was funded by SNF Ambizione grant PZ00P3_193646. We also appreciate the FLUXNET in providing the valuable measurements.

Author contributions: C.W. proposed the original idea. C.W. M.G. and Q.G. designed the research. C.W., J.W., C.M.Z., J.P., and P.F. wrote the first draft of the manuscript. J.W. and L.D. performed the ground and remote sensing data analysis. J.W. and H.H. performed model simulation analysis. L.D. performed the meta-analysis. H.H. performed eddy-covariance flux data analysis. D.L. performed the experimental analysis. J.W. generated the remote sensing $PM_{2.5}$ data. All authors contributed to the writing of the manuscript.

Competing interests: Authors declare that they have no competing interests.

Data and materials availability: All data are available in the supplementary materials. The specific link for each dataset can be found in the Supplementary Table 1. All the data analyses were performed using MATLAB or R.

References

1. Piao, S. *et al.* Characteristics, drivers and feedbacks of global greening. *Nat Rev Earth Environ* **1**, 14–27 (2020).
2. Zhu, Z. *et al.* Greening of the Earth and its drivers. *Nature Clim Change* **6**, 791–795 (2016).
3. Peñuelas, J., Rutishauser, T. & Filella, I. Phenology Feedbacks on Climate Change. *Science* **324**, 887–888 (2009).
4. Wang, J. *et al.* Large Chinese land carbon sink estimated from atmospheric carbon dioxide data. *Nature* **586**, 720–723 (2020).
5. Song, X.-P. *et al.* Global land change from 1982 to 2016. *Nature* **560**, 639–643 (2018).
6. Keenan, T. F. *et al.* Net carbon uptake has increased through warming-induced changes in temperate forest phenology. *Nature Clim Change* **4**, 598–604 (2014).
7. Walther, G.-R. *et al.* Ecological responses to recent climate change. *Nature* **416**, 389–395 (2002).
8. Fu, Y. H. *et al.* Declining global warming effects on the phenology of spring leaf unfolding. *Nature* **526**, 104–107 (2015).
9. Wu, C. *et al.* Interannual variability of net ecosystem productivity in forests is explained by carbon flux phenology in autumn: Autumn phenology and NEP. *Global Ecology and Biogeography* **22**, 994–1006 (2013).
10. Jeong, S.-J., Ho, C.-H., Gim, H.-J. & Brown, M. E. Phenology shifts at start vs. end of growing season in temperate vegetation over the Northern Hemisphere for the period 1982-2008: phenology shifts at start vs. end of growing. *Global Change Biology* **17**, 2385–2399 (2011).
11. Huang, K. *et al.* Enhanced peak growth of global vegetation and its key mechanisms. *Nat Ecol Evol* **2**, 1897–1905 (2018).
12. Wu, C. *et al.* Contrasting responses of autumn-leaf senescence to daytime and night-time warming. *Nature Clim Change* **8**, 1092–1096 (2018).
13. Myneni, R. B., Keeling, C. D., Tucker, C. J., Asrar, G. & Nemani, R. R. Increased plant growth in the northern high latitudes from 1981 to 1991. *Nature* **386**, 698–702 (1997).
14. Chen, C. *et al.* China and India lead in greening of the world through land-use management. *Nat Sustain* **2**, 122–129 (2019).
15. Yue, H., He, C., Huang, Q., Yin, D. & Bryan, B. A. Stronger policy required to substantially reduce deaths from $PM_{2.5}$ pollution in China. *Nat Commun* **11**, 1462 (2020).
16. Xu, R. *et al.* Global population exposure to landscape fire air pollution from 2000 to 2019. *Nature* **621**, 521–529 (2023).

17. Burke, M. *et al.* The contribution of wildfire to $PM_{2.5}$ trends in the USA. *Nature* **622**, 761–766 (2023).
18. Geng, G. *et al.* Drivers of $PM_{2.5}$ air pollution deaths in China 2002–2017. *Nat. Geosci.* **14**, 645–650 (2021).
19. Barlow, J. *et al.* Anthropogenic disturbance in tropical forests can double biodiversity loss from deforestation. *Nature* **535**, 144–147 (2016).
20. Inness, A. *et al.* The CAMS reanalysis of atmospheric composition. *Atmos. Chem. Phys.* **19**, 3515–3556 (2019).
21. Friedl, M., Gray, J. & Sulla-Menashe, D. MCD12Q2 MODIS/Terra+Aqua Land Cover Dynamics Yearly L3 Global 500m SIN Grid V006. (2019) doi:10.5067/MODIS/MCD12Q2.006.
22. Zhang, Y., Joiner, J., Alemohammad, S. H., Zhou, S. & Gentine, P. A global spatially contiguous solar-induced fluorescence (CSIF) dataset using neural networks. *Biogeosciences* **15**, 5779–5800 (2018).
23. Jbaily, A. *et al.* Air pollution exposure disparities across US population and income groups. *Nature* **601**, 228–233 (2022).
24. Holmes, C. D. Air pollution and forest water use. *Nature* **507**, E1–E2 (2014).
25. Liang, X. *et al.* Stomatal responses of terrestrial plants to global change. *Nat Commun* **14**, 2188 (2023).
26. Li, Y., Wang, Y., Wang, B., Wang, Y. & Yu, W. The Response of Plant Photosynthesis and Stomatal Conductance to Fine Particulate Matter ($PM_{2.5}$) based on Leaf Factors Analyzing. *J. Plant Biol.* **62**, 120–128 (2019).
27. Xu, J., Hu, W., Liang, D. & Gao, P. Photochemical impacts on the toxicity of PM $_{2.5}$. *Critical Reviews in Environmental Science and Technology* **52**, 130–156 (2022).
28. Wang, Y., Wang, Y., Tang, Y. & Zhu, X.-G. Stomata conductance as a goalkeeper for increased photosynthetic efficiency. *Current Opinion in Plant Biology* **70**, 102310 (2022).
29. Yao, L. *et al.* Co-benefits of reducing $PM_{2.5}$ and improving visibility by COVID-19 lockdown in Wuhan. *npj Clim Atmos Sci* **4**, 40 (2021).
30. Kalashnikov, D. A., Schnell, J. L., Abatzoglou, J. T., Swain, D. L. & Singh, D. Increasing co-occurrence of fine particulate matter and ground-level ozone extremes in the western United States. *Sci. Adv.* **8**, eabi9386 (2022).
31. Rap, A. *et al.* Enhanced global primary production by biogenic aerosol via diffuse radiation fertilization. *Nature Geosci* **11**, 640–644 (2018).
32. Quinn Thomas, R., Canham, C. D., Weathers, K. C. & Goodale, C. L. Increased tree carbon storage in response to nitrogen deposition in the US. *Nature Geosci* **3**, 13–17 (2010).
33. Liu, X. *et al.* Enhanced nitrogen deposition over China. *Nature* **494**, 459–462 (2013).
34. Persad, G. G. & Caldeira, K. Divergent global-scale temperature effects from identical aerosols emitted in different regions. *Nat Commun* **9**, 3289 (2018).

35. Watson-Parris, D. & Smith, C. J. Large uncertainty in future warming due to aerosol forcing. *Nat. Clim. Chang.* **12**, 1111–1113 (2022).
36. Wei, J. *et al.* Long-term mortality burden trends attributed to black carbon and $PM_{2.5}$ from wildfire emissions across the continental USA from 2000 to 2020: a deep learning modelling study. *The Lancet Planetary Health* **7**, e963–e975 (2023).
37. Wei, J. *et al.* First close insight into global daily gapless 1 km $PM_{2.5}$ pollution, driving factors, and health impact. https://www.researchsquare.com/article/rs-2626358/v1 (2023) doi:10.21203/rs.3.rs-2626358/v1.
38. Wang, Z. *et al.* Modeling study of regional severe hazes over mid-eastern China in January 2013 and its implications on pollution prevention and control. *Sci. China Earth Sci.* **57**, 3–13 (2014).
39. Chen, J. *et al.* A simple method for reconstructing a high-quality NDVI time-series data set based on the Savitzky–Golay filter. *Remote Sensing of Environment* **91**, 332–344 (2004).
40. Ma, H. & Liang, S. Development of the GLASS 250-m leaf area index product (version 6) from MODIS data using the bidirectional LSTM deep learning model. *Remote Sensing of Environment* **273**, 112985 (2022).
41. He, L. *et al.* The weekly cycle of photosynthesis in Europe reveals the negative impact of particulate pollution on ecosystem productivity. *Proc. Natl. Acad. Sci. U.S.A.* **120**, e2306507120 (2023).
42. Sitch, S. *et al.* Recent trends and drivers of regional sources and sinks of carbon dioxide. *Biogeosciences* **12**, 653–679 (2015).
43. Friedlingstein, P. *et al.* Global Carbon Budget 2023. *Earth System Science Data* **15**, 5301–5369 (2023).
44. Abatzoglou, J. T., Dobrowski, S. Z., Parks, S. A. & Hegewisch, K. C. TerraClimate, a high-resolution global dataset of monthly climate and climatic water balance from 1958–2015. *Sci Data* **5**, 170191 (2018).
45. Brown, J. ,. O. Ferrians, J. A. Heginbottom & Melnikov, E. Circum-Arctic Map of Permafrost and Ground-Ice Conditions, Version 2. (2002) doi:10.7265/skbg-kf16.
46. Freer-Smith, P. H., El-Khatib, A. A. & Taylor, G. Capture of Particulate Pollution by Trees: A Comparison of Species Typical of Semi-Arid Areas (Ficus Nitida and Eucalyptus Globulus) with European and North American Species. *Water, Air, & Soil Pollution* **155**, 173–187 (2004).
47. Liang, D., Ma, C., Wang, Y., Wang, Y. & Chen-xi, Z. Quantifying $PM_{2.5}$ capture capability of greening trees based on leaf factors analyzing. *Environ Sci Pollut Res* **23**, 21176–21186 (2016).
48. Norby, R. J., Cotrufo, M. F., Ineson, P., O'Neill, E. G. & Canadell, J. G. Elevated CO2, litter chemistry, and decomposition: a synthesis. *Oecologia* **127**, 153–165 (2001).
49. Rustad, L. *et al.* A meta-analysis of the response of soil respiration, net nitrogen mineralization, and aboveground plant growth to experimental ecosystem warming. *Oecologia* **126**, 543–562 (2001).
50. Koricheva, J. & Gurevitch, J. Uses and misuses of meta-analysis in plant ecology. *J Ecol* **102**, 828–844 (2014).

51. Van Groenigen, K. J., Osenberg, C. W. & Hungate, B. A. Increased soil emissions of potent greenhouse gases under increased atmospheric CO2. *Nature* **475**, 214–216 (2011).
52. Pittelkow, C. M. *et al.* Productivity limits and potentials of the principles of conservation agriculture. *Nature* **517**, 365–368 (2015).
53. *Handbook of Meta-analysis in Ecology and Evolution*. (Princeton University Press, 2013). doi:10.1515/9781400846184.
54. Viechtbauer, W. Conducting Meta-Analyses in *R* with the **metafor** Package. *J. Stat. Soft.* **36**, (2010).
55. Li, J. *et al.* An Algorithm Differentiating Sunlit and Shaded Leaves for Improving Canopy Conductance and Vapotranspiration Estimates. *J. Geophys. Res. Biogeosci.* **124**, 807–824 (2019).
56. *Crop evapotranspiration: guidelines for computing crop water requirements*. (Food and Agriculture Organization of the United Nations, 1998).
57. Monteith, J. L. & Unsworth, M. H. *Principles of environmental physics: plants, animals, and the atmosphere*. (Elsevier/Academic Press, 2013).
58. Yebra, M., Van Dijk, A., Leuning, R., Huete, A. & Guerschman, J. P. Evaluation of optical remote sensing to estimate actual evapotranspiration and canopy conductance. *Remote Sensing of Environment* **129**, 250–261 (2013).
59. Lu, X. *et al.* Maximum Carboxylation Rate Estimation With Chlorophyll Content as a Proxy of Rubisco Content. *J. Geophys. Res. Biogeosci.* **125**, (2020).
60. Ryu, Y., Jiang, C., Kobayashi, H. & Detto, M. MODIS-derived global land products of shortwave radiation and diffuse and total photosynthetically active radiation at 5 km resolution from 2000. *Remote Sensing of Environment* **204**, 812–825 (2018).
61. Chen, J. M. *et al.* Vegetation structural change since 1981 significantly enhanced the terrestrial carbon sink. *Nat Commun* **10**, 4259 (2019).
62. Bagozzi, R. P. & Yi, Y. Specification, evaluation, and interpretation of structural equation models. *J. of the Acad. Mark. Sci.* **40**, 8–34 (2012).
63. Rosseel, Y. **lavaan**: An *R* Package for Structural Equation Modeling. *J. Stat. Soft.* **48**, (2012).

Figures

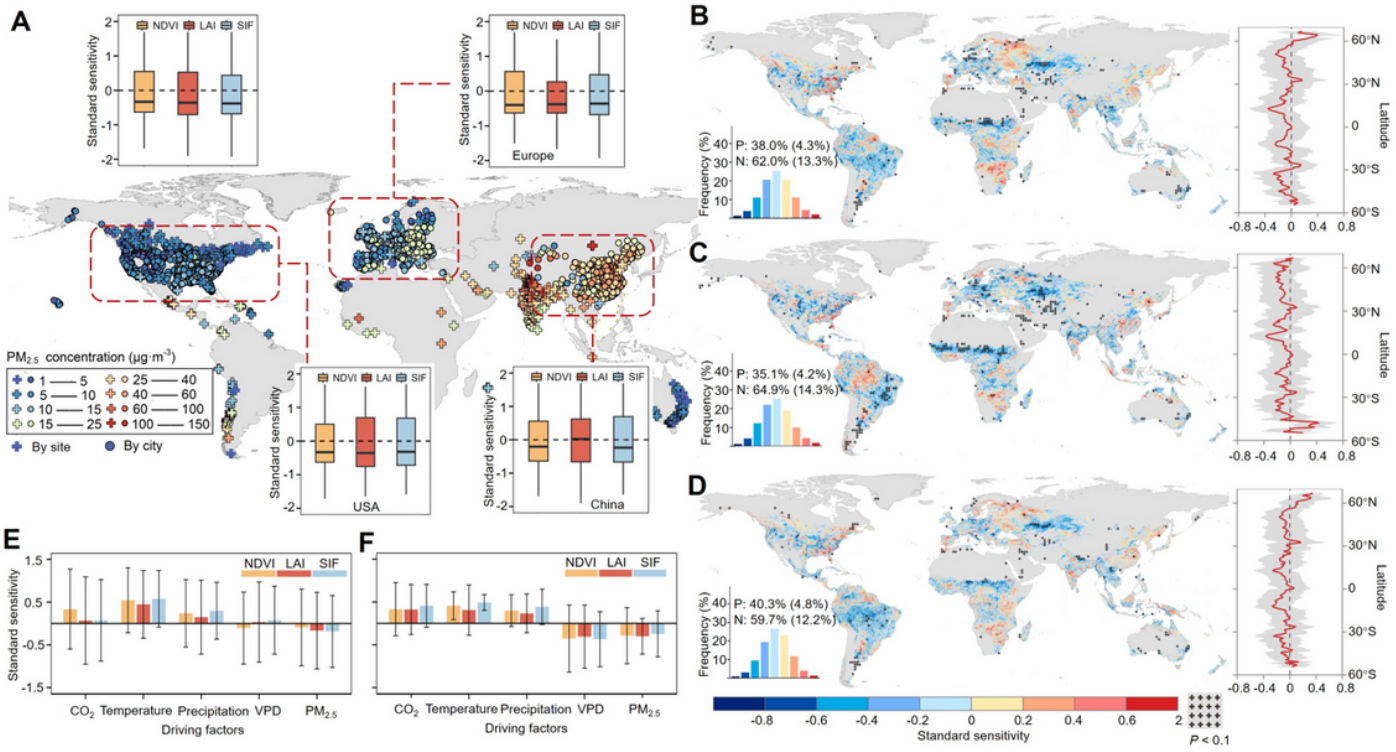

Figure 1

Spring greening sensitivity to $PM_{2.5}$ air pollution from site to global scales. A, The standard sensitivity (Supplementary Materials and Methods) of spring greening indicators (i.e., NDVI, LAI, and SIF) to ground-observed $PM_{2.5}$ pollution for the globe (upper-left boxplot) and regions (i.e., Europe, USA, and China). The crosses and points with colors indicate local level of $PM_{2.5}$ pollution. **B-D,** The standard sensitivity of spring greening indicators (i.e., **B:** NDVI, **C:** LAI, **D:** SIF) to satellite-observed $PM_{2.5}$ pollution from 2000 to 2020. The right panels represent variations of standard sensitivity along with latitude gradients. **E, F,** The standard sensitivities of spring greening indicators to driving factors, i.e., CO_2, temperature, precipitation, VPD, and $PM_{2.5}$ pollution, at site (**E**) and global (**F**) scales.

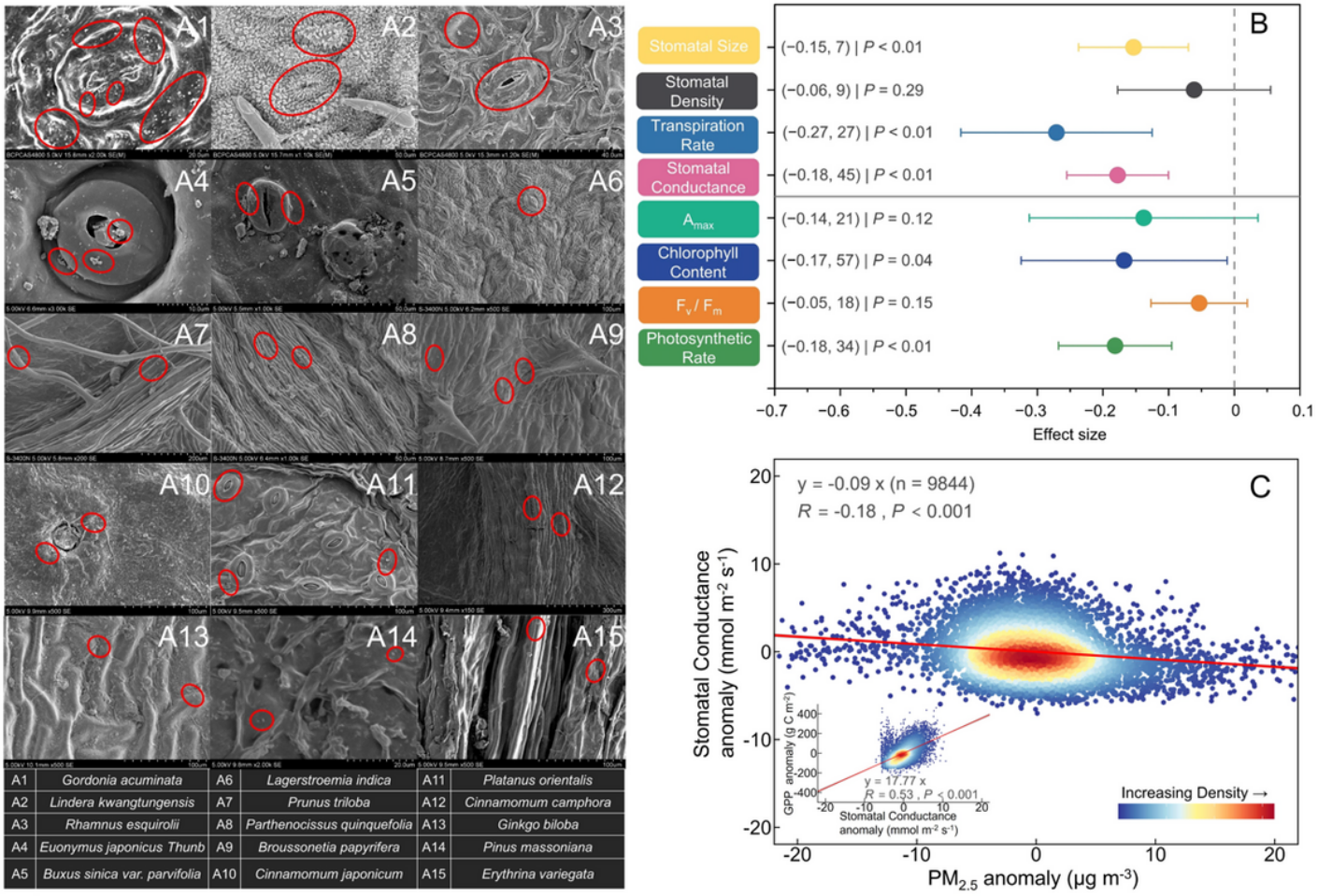

A1	*Gordonia acuminata*	A6	*Lagerstroemia indica*	A11	*Platanus orientalis*
A2	*Lindera kwangtungensis*	A7	*Prunus triloba*	A12	*Cinnamomum camphora*
A3	*Rhamnus esquirolii*	A8	*Parthenocissus quinquefolia*	A13	*Ginkgo biloba*
A4	*Euonymus japonicus Thunb*	A9	*Broussonetia papyrifera*	A14	*Pinus massoniana*
A5	*Buxus sinica var. parvifolia*	A10	*Cinnamomum japonicum*	A15	*Erythrina variegata*

Figure 2

Observational evidence of the impacts of $PM_{2.5}$ pollution on leaf morphology, gas exchange and photosynthesis. A1-A15, Leaf morphology of 15 tree species exposed to $PM_{2.5}$ pollution (Supplementary Table 2). The red circle highlights the $PM_{2.5}$ particles adhering to the leaf surface, potentially causing blockage and damage to leaf stomata. **B**, The effect of $PM_{2.5}$ on plant physiological indicators related to gas exchange and photosynthesis (Supplementary Table 3). A_{max} represents the maximum rate of carbon assimilation, and F_v/F_m represents the maximum quantum efficiency of Photosystem Π. The values in brackets represent the mean effect size (left) and number of species (right) in each estimate. *P*-values are shown when the effect size of a variable is significant ($P < 0.05$). **C**, The relationship between the monthly anomalies of $PM_{2.5}$ and stomatal conductance derived from global flux measurements (Supplementary Table 4). The subplot shows the relationship between anomalies of stomatal conductance and gross primary productivity (GPP).

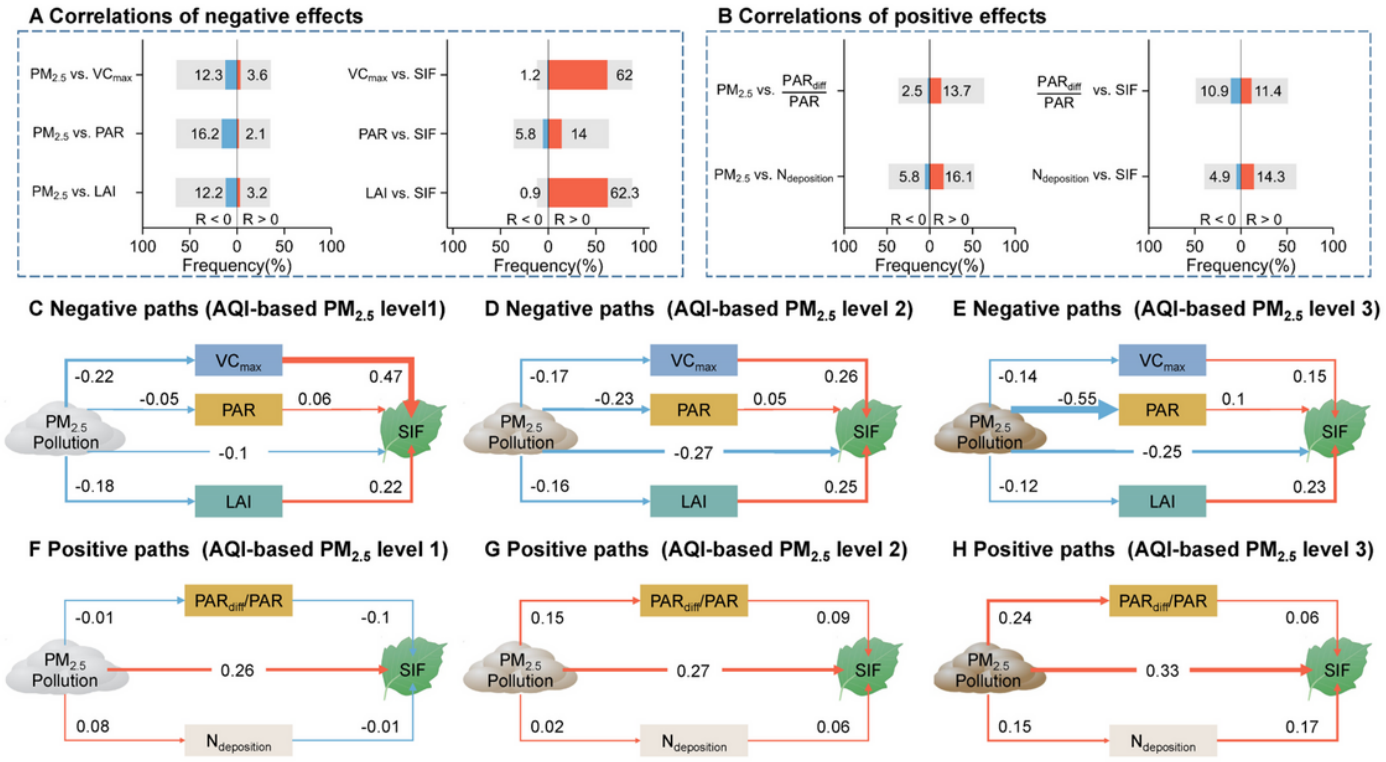

Figure 3

Potential mechanisms underlying the correlation between spring photosynthesis (i.e., SIF) and $PM_{2.5}$ pollution. A, Correlation of negative effects of $PM_{2.5}$ emissions. The maximum rate of carboxylation (VC_{max}), photosynthetically active radiation (PAR), and LAI were considered to link $PM_{2.5}$ and SIF. **B,** Correlation of positive effects of $PM_{2.5}$ emissions. The fraction of diffuse radiation (PAR_{diff}/PAR) and nitrogen deposition ($N_{deposition}$) were considered to link $PM_{2.5}$ and SIF. **C-H**, Structural equation model describing the biogeophysical and biogeochemical relationships between $PM_{2.5}$ emissions and SIF for negative (**C-E**) and positive paths (**F-H**) based on three levels of AQI-based $PM_{2.5}$ (Supplementary Materials and Methods).

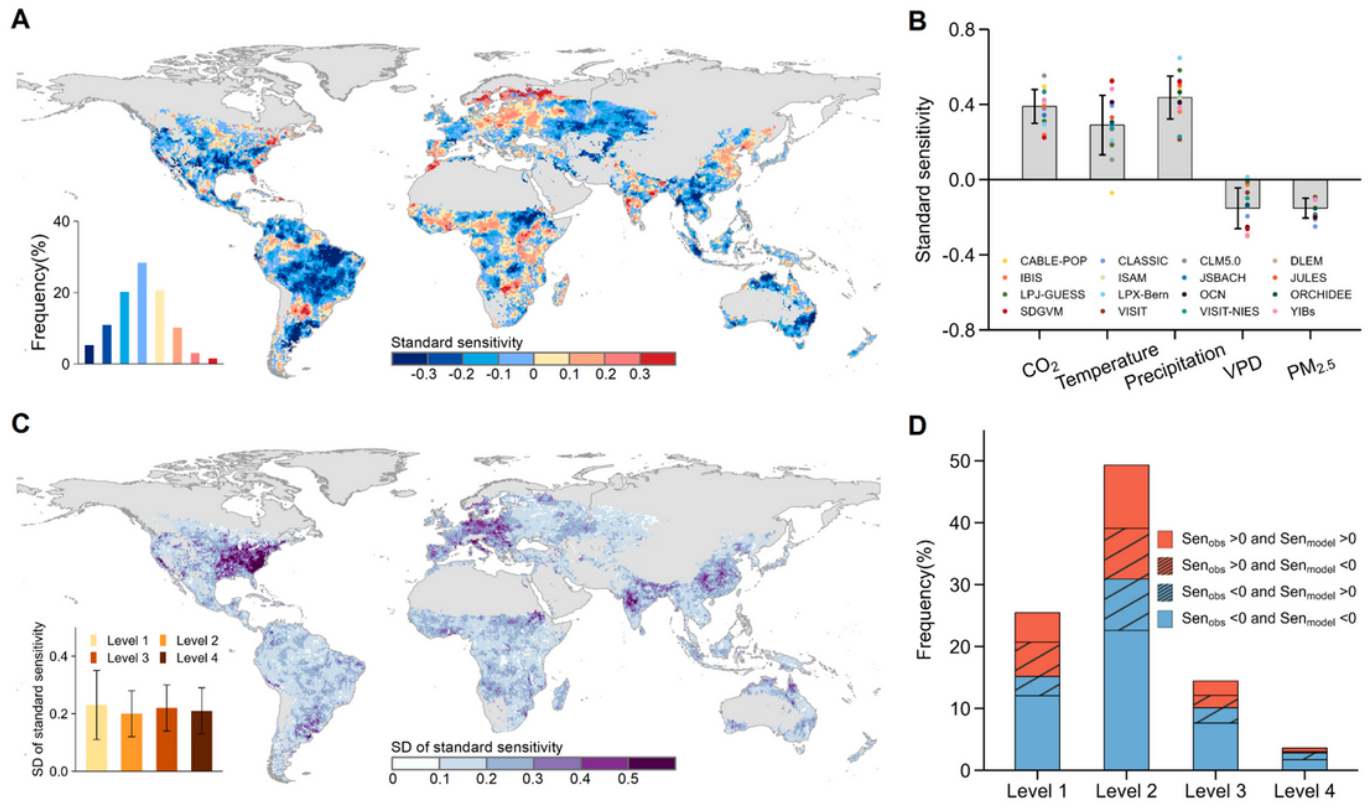

Figure 4

Effects of $PM_{2.5}$ pollution on spring productivity stimulated by state-of-the-art terrestrial ecosystem models. A, C, The mean (**A**) and standard deviation (SD) (**C**) of standard sensitivity of spring gross primary productivity (GPP), generated by 16 ecosystem models (Table S5), to $PM_{2.5}$ pollution. **B**, The standard sensitivity of spring GPP to driving factors, including CO_2, temperature, precipitation, vapor pressure deficit (VPD), and $PM_{2.5}$. **D**, The consistency of $PM_{2.5}$ effect in direction between model- (Sen_{model}) and satellite-observation-based (Sen_{obs}) analyses at four levels of AQI-based $PM_{2.5}$.

Supplementary Files

This is a list of supplementary files associated with this preprint. Click to download.

- PM2.5NatureSI.docx
- ExtendedData.docx